Topological charge pump by surface acoustic waves*

Yi Zheng(郑一), Shi-Ping Feng(冯世平), and Shi-Jie Yang(杨师杰)†

Department of Physics, Beijing Normal University, Beijing 100875, *China*

(Received 22 September 2015; revised manuscript received 3 March 2016; published online 20 April 2016)

Quantized electron pumping by the surface acoustic wave across barriers created by a sequence of split metal gates is interpreted from the viewpoint of topology. The surface acoustic wave serves as a one-dimensional periodical potential whose energy spectrum possesses the Bloch band structure. The time-dependent phase plays the role of an adiabatic parameter of the Hamiltonian which induces a geometrical phase. The pumping currents are related to the Chern numbers of the filled bands below the Fermi energy. Based on this understanding, we predict a novel effect of quantized but non-monotonous current plateaus simultaneously pumped by two homodromous surface acoustic waves.

Keywords: quantized pumping, surface acoustic wave, topological band structure

PACS: 73.20.At, 73.21.Hb, 72.50.+b **DOI:** 10.1088/1674-1056/25/6/067301

1. Introduction

The surface acoustic wave (SAW) is frequently used as an experimental tool to transport electrons in one-dimensional (1D) quantum lines as well as in two-dimensional electron gases (2DEGs).[1,2] The SAW experiments in the 1D channel on GaAs-$Al_xGa_{1-x}As$ heterojunctions reveal quantized plateaus of acoustic-electric current which are proportional to the frequency of the acoustic wave, $I = n \cdot ef$ (n is an integer).[3] It means that an integer number of electrons are pumped through the channel in one oscillating cycle of the SAW. A lot of theoretical works have attempted to interpret this quantum phenomenon.[4–7] It is intuitively considered that the Coulomb-blockade effect may play a key role. The explicit mechanism, however, remains controversial. In Ref. [8], the authors discussed the precision of the plateaus and impurity of the potentials. Other works of modeling the quantized pump are based on the tight-binding model which consists of discrete quantum dots and two leads connecting the electron reservoirs on each side. The non-interacting electron transportation is expressed by reduced nearest-neighbor hopping amplitudes.[9,10] This model is analogous to the discrete 1D Harper model which exhibits a non-trivial topological phase.[11]

Topology as a mathematical conception has been serving the condensed matter physics for 30 years since the explanation of the quantized Hall effects. It has become a useful means in understanding the topological insulator,[12] superconductivity,[13–15] and the quantized charge or spin pump.[16,17] It has been implemented in optical lattices[18,19] and in graphene-like materials as well.[20,21] In this paper, we propose a setup with a sequence of split metal gates in the 1D channel, creating a sequence of barrier potentials. We then explore the topology implications of the quantized charge pumping by a SAW within the band theory. In the quantized charge pumping process, the electrons follow an adiabatically varying potential.[22] The surface acoustic wave is taken as a spatially periodical potential whose energy spectrum possesses the Bloch band structure, whereas the time-dependent phase plays the role of an adiabatic parameter of the Hamiltonian which induces a geometrical phase. The staircase-like acoustic currents are characterized by topological Chern numbers. We investigate the dependence of the number of pumped electrons on physical parameters such as the height of the barrier, the amplitude of the SAW and the Fermi levels and reveal a series of topological transitions. Based on this interpretation, we further predict a novel effect of quantized but non-monotonous current plateaus simultaneously pumped by two homodromous SAWs.

2. Model and band topology

The 1D narrow channel was experimentally realized by a split metal gate on the surface of a GaAs-$Al_xGa_{1-x}As$ heterojunction. The time-dependent SAW potential induced by the piezoelectric effects is written as

$$\tilde{V}(x,t) = V_{\mathrm{SAW}} \cos^2(q\pi x/a - \omega t) \tag{1}$$

with V_{SAW} the amplitude. To study the topological properties of the quantum pumping process, we suppose the 1D channel contains a sequence of split metal gates, with a the length of a gate and q the number of spatial periods of the SAW in a single gate. Each split gate is modeled typically by a Gaussian-like barrier potential,[23]

$$V_{\mathrm{g}}(x) = \frac{V_0}{\cosh^2[(x-a/2)/\sigma]}, \tag{2}$$

*Project supported by the National Natural Science Foundation of China (Grant No. 11374036) and the National Basic Research Program of China (Grant No. 2012CB821403).

†Corresponding author. E-mail: yangshijie@tsinghua.org.cn

© 2016 Chinese Physical Society and IOP Publishing Ltd

where the parameter σ specifies the width of a barrier which is set to $\sigma = a/4$ in our model. Experimentally, V_g is controlled by the gate voltage applied to the 1D channel. We treat the static barrier potential in the q-period of the SAW ($0 < x < a$) by making use of the periodical condition. The time-dependent Hamiltonian reads:

$$\hat{H}(x,t) = -\frac{\hbar^2}{2m}\frac{\mathrm{d}^2}{\mathrm{d}x^2} + V_g(x) + \tilde{V}(x,t) \tag{3}$$

with $\hat{H}(x+a,t) = \hat{H}(x,t)$.

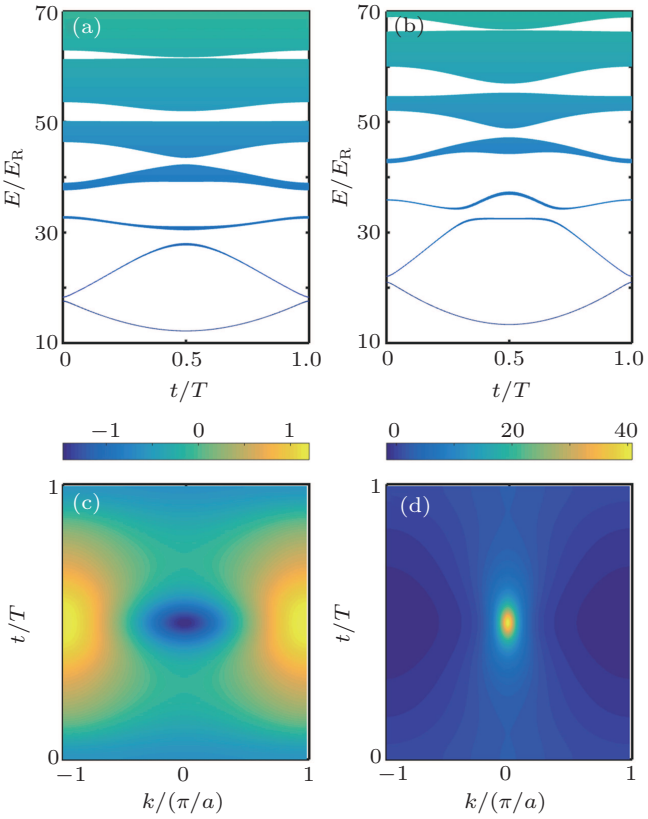


Fig. 1. (color online) Energy band structure of E versus time t for (a) $V_0 = 20E_R$ and (b) $V_0 = 30E_R$. The amplitude of the SAW is fixed as $V_{SAW} = 30E_R$ and $q = 2$. Panel (b) shows that a band crossing occurs between the 2nd and 3rd bands as V_0 increases. Panels (c) and (d) are the topographical maps of the Berry curvature distributions for the 3rd and 4th bands at $V_0 = 20E_R$. The integrations over the BZ give rise to the Chern number of 0 and 1, respectively.

For the slowly oscillating SAW, the system can be treated as a quasi-static problem. The time-dependent phase $\delta = \omega t$ is taken as a variable parameter that yields a Berry phase as δ changes to complete a cycle from 0 to π. The Bloch wave vector k is approximately a good quantum number at a given δ. The periodicity both in the k-space and the δ-space defines a 2D Brillouin zone (BZ). In the upper row of Fig. 1 we display the energy band structures versus the time or δ for two values of barrier height (a) $V_0 = 20E_R$ and (b) $V_0 = 30E_R$ at a fixed SAW amplitude $V_{SAW} = 30E_R$. Here $E_R = \hbar^2\pi^2/2ma^2$ is taken as the unit of energy. The dependence of E on the Bloch momentum k leads to broadening of the energy bands and the gaps vary with time. By comparing band structures shown in Figs. 1(a) and 1(b) which are plotted in the periodic scheme, we note that as V_0 increases, the energy gaps may close and reopen and level crossings take place between the adjacent bands.

The Berry curvature of a given band in the torus-shape BZ is defined as

$$\Omega^n_{k,t} = \mathrm{i}\left[\left\langle \frac{\partial u_n}{\partial k} \middle| \frac{\partial u_n}{\partial t} \right\rangle - \mathrm{c.c.}\right], \tag{4}$$

where n is the band index. The lower row of Fig. 1 shows the topographical map of the Berry curvature versus k and t for (c) $n = 2$ and (d) $n = 3$ energy bands in panel (a). The topology of a single band is characterized by a Chern number which is the integration of the Berry curvature over the BZ,[24]

$$C_n = \frac{1}{2\pi}\int_{\mathrm{BZ}} \Omega^n_{k,t}\,\mathrm{d}k\,\mathrm{d}t. \tag{5}$$

The Chern number of each band can be computed as long as they are well-separated. For example, the integrations of Berry curvature distributions in Figs. 1(c) and 1(d) give a Chern number of 0 and 1, respectively.

Table 1. Chern numbers C_n of the six lowest energy bands for various values of V_0. The amplitude of the SAW is fixed at $V_{SAW} = 30E_R$. The slashes indicate that the Chern numbers are not well-defined due to closing of the gap.

$V_0(E_R)$	10	20	30	40	50	60	70
C_1	0	0	0	0	0	0	0
C_2	1	1	0	0	0	0	0
C_3	0	0	1	1	0	0	0
C_4	1	1	0	0	1	1	0
C_5	/	0	1	1	0	0	1
C_6	/	/	0	0	1	1	0

Table 1 lists the Chern numbers of the six lowest bands versus V_0 for the model Hamiltonian (3) with $q = 2$. The amplitude of the SAW is fixed at $V_{SAW} = 30E_R$. The Chern numbers for $V_0 = 0$ are not shown, where the eigen equation is simply the Harper equation and the model is a sliding lattice. Each pair of adjacent bands corresponds to a single band of the $V_0 = 0$ model, e.g., $C_1 + C_2$ instead of C_1 or C_2 separately is well-defined. The change of V_0 opens or closes a gap, leading to jumps of the Chern number or topological transitions of the bands.

3. Topological transition and quantized pumping

We examine the relation of the band topology with the system parameters. Figure 2 plots the six lowest gaps versus V_0 at different times $\omega t = 0, \pi/8, \pi/4, 3\pi/8$, and $\pi/2$, respectively. The amplitude of the SAW potential is $V_{SAW} = 30E_R$. From Fig. 2(b) we observe that the second energy gap is closed and reopened at $V_0/E_R \simeq 24$, which corresponds to the jump of the Chern number in C_2 and C_3 as displayed in Table 1. It

implies that a topological transition occurs. The same transitions occur in the third gap at $V_0/E_R \simeq 43$ (Fig. 2(c)), in the fourth gap at $V_0^{A_1}/E_R \simeq 24$ and $V_0^{A_2}/E_R \simeq 64$ (Fig. 2(d)), and in the fifth gap at $V_0^{A_1}/E_R \simeq 46$ and $V_0^{A_2}/E_R \simeq 78$ (Fig. 2(e)), respectively. The topological transition points are intimately related to the closing points of the energy gaps.

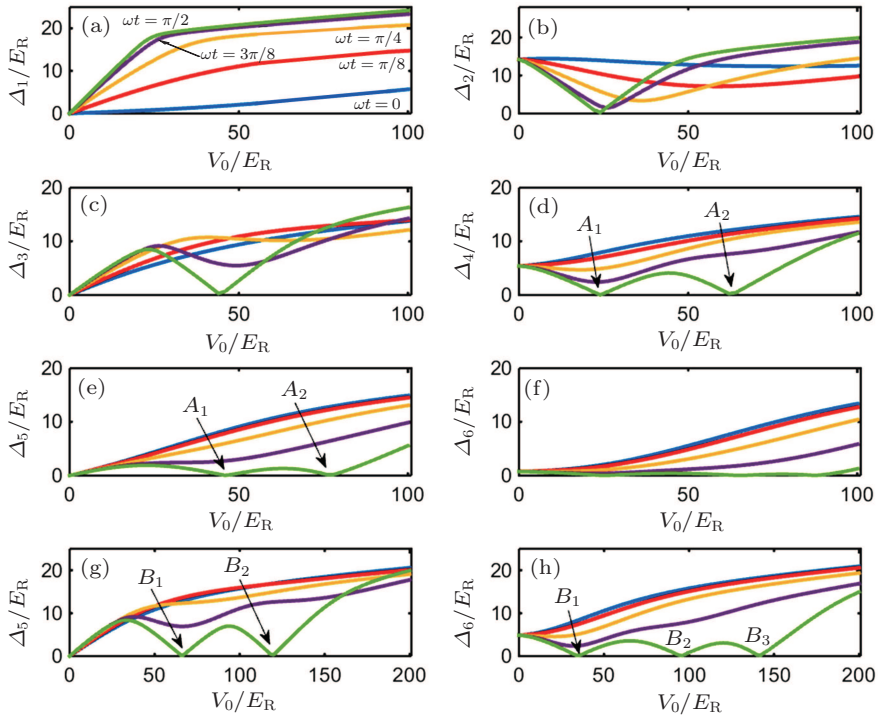


Fig. 2. (color online) Energy gaps Δ_n versus the amplitudes V_0 of the barrier potential at different time points $\omega t = 0$ (blue), $\pi/8$ (red), $\pi/4$ (yellow), $3\pi/8$ (purple), $\pi/2$ (green). Panels (a)–(f) correspond to $n = 1$–6 gaps with $V_{SAW} = 30E_R$. The zeros of the curves indicate that the gaps vanish. As a comparison, panels (g) and (h) respectively illustrate Δ_5 and Δ_6 for a larger SAW amplitude $V_{SAW} = 60E_R$ where the 6th gap is reopened because of nonzero Δ_6. It means that the amplitude of the SAW modifies the topology of the energy bands.

On the other hand, topological transitions can also be implemented by adjusting the SAW amplitude V_{SAW}. As V_{SAW} increase from $30E_R$ (Fig. 2(f)) to $60E_R$ (Fig. 2(h)), gap-closing points appear at B_1, B_2, and B_3. To give a complete description of the relations of the band topology with the system parameters, we show in Fig. 3 the topographical map of the minimum gaps in the time period versus V_0 and V_{SAW}. The horizontal lines A and B in Figs. 3(e) and 3(f) mark $V_{SAW} = 30E_R$ and $V_{SAW} = 60E_R$, respectively. The crossing points A_1, A_2, and B_1 and B_2 in Fig. 3(e) correspond to the transition points in Figs. 2(e) and 2(g). Accordingly, the points B_1, B_2, and B_3 in Fig. 3(f) correspond to the transition points in Fig. 2(h).

For the particle pumping, we adopt the adiabatic approximation analysis of the geometric phase[25–27] by considering that the velocity of the acoustic wave is much smaller than the Fermi velocity,[28,29]

$$|\psi_t\rangle = e^{i\gamma_n} \exp\left[-\frac{i}{\hbar}\int_{t_0}^{t} dt' E_n(t')\right] \times \left[|u_n\rangle - i\hbar \sum_{n\neq n'} \frac{|u_{n'}\rangle\langle u_{n'}|\partial_t|u_n\rangle}{E_n - E_{n'}}\right]. \quad (6)$$

It satisfies the time-dependent Schrödinger equation $i\hbar\partial_t|\psi_t\rangle = \hat{H}(t)|\psi_t\rangle$. We have used the instantaneous eigenstates (the Bloch states) $|u_n\rangle$ of the Hamiltonian $\hat{H}(t)$ and $\gamma_n = i\int_{t_0}^{t} dt' \langle u_n|\partial_{t'}|u_n\rangle$. The system has a complete temporal dependence on the SAW potential, which is periodically varying with the period $T = \pi/\omega$. The expectation of the velocity operator $\hat{v}_n = \partial H(k,t)/\partial(\hbar k)$ is

$$\begin{aligned}\langle v_n(k)\rangle &= \langle\psi_t|\hat{v}_n|\psi_t\rangle \\ &= \frac{\partial E_n}{\hbar\partial k} - i\times\sum_{n\neq n'}\left[\frac{\langle u_n|\partial H/\partial k|u_{n'}\rangle\langle u_{n'}|\partial_t|u_n\rangle}{E_n - E_{n'}}\right] \\ &= \frac{\partial E_n(k)}{\hbar\partial k} - \Omega^n_{k,t}. \end{aligned} \quad (7)$$

The last equivalence is obtained by making use of the relation $\langle u_n|\partial H/\partial k|u_{n'}\rangle = (E_n - E_{n'})\langle\partial u_n/\partial k|u_{n'}\rangle$. Here insulating states rather than conducting states contribute to the induced current, thus only initially full-filled bands are of concern. The pumping current is the integration of $\langle v_n(k)\rangle$ over the BZ, in which the zeroth-order term vanishes. The total number of particles pumped in an oscillating cycle is

$$Q_n = i\int_0^T dt \int_{BZ} \frac{dk}{2\pi}\left[\langle\partial_t u_n|\partial_k u_n\rangle - \langle\partial_k u_n|\partial_t u_n\rangle\right]. \quad (8)$$

This is exactly the Chern number calculated from formulism (5). It demonstrates that the adiabatic pumping is quantized and the total number of pumped particles is equal to the summation of the Chern numbers of all completely filled bands. Thus the Fermi level should also be considered to determine the amount of bands that are of concern.

For example, if the lowest four bands are occupied, there are two transition points A_1 and A_2 in Fig. 2(d) as V_0 increases. We notice that $V_0^{A_1}$ is also the transition point of the second gap, as shown in Fig. 2(b). Consequently, there exist two quantized current plateaus. In the same way, the two transition points A_1 and A_2 in Fig. 2(e) indicate three current plateaus of $I = 2ef$ for $0 \le V_0 < V_0^{A_1}$, $I = 1ef$ for $V_0^{A_1} < V_0 < V_0^{A_2}$, and $I = 0$ for $V_0^{A_2} < V_0$. Here $f = \omega/\pi$ is the frequency of the SAW. In order to obtain higher current plateaus, one just needs to implement a larger SAW amplitude in which more electrons are classically trapped in a spatial period. In our frame of analysis, we need more transition points in the well-separated gaps, as the transition points B_1, B_2, and B_3 in the fifth (Fig. 2(g)) and sixth gaps (Fig. 2(h)) for a larger SAW amplitude $V_{\rm SAW} = 60E_{\rm R}$.

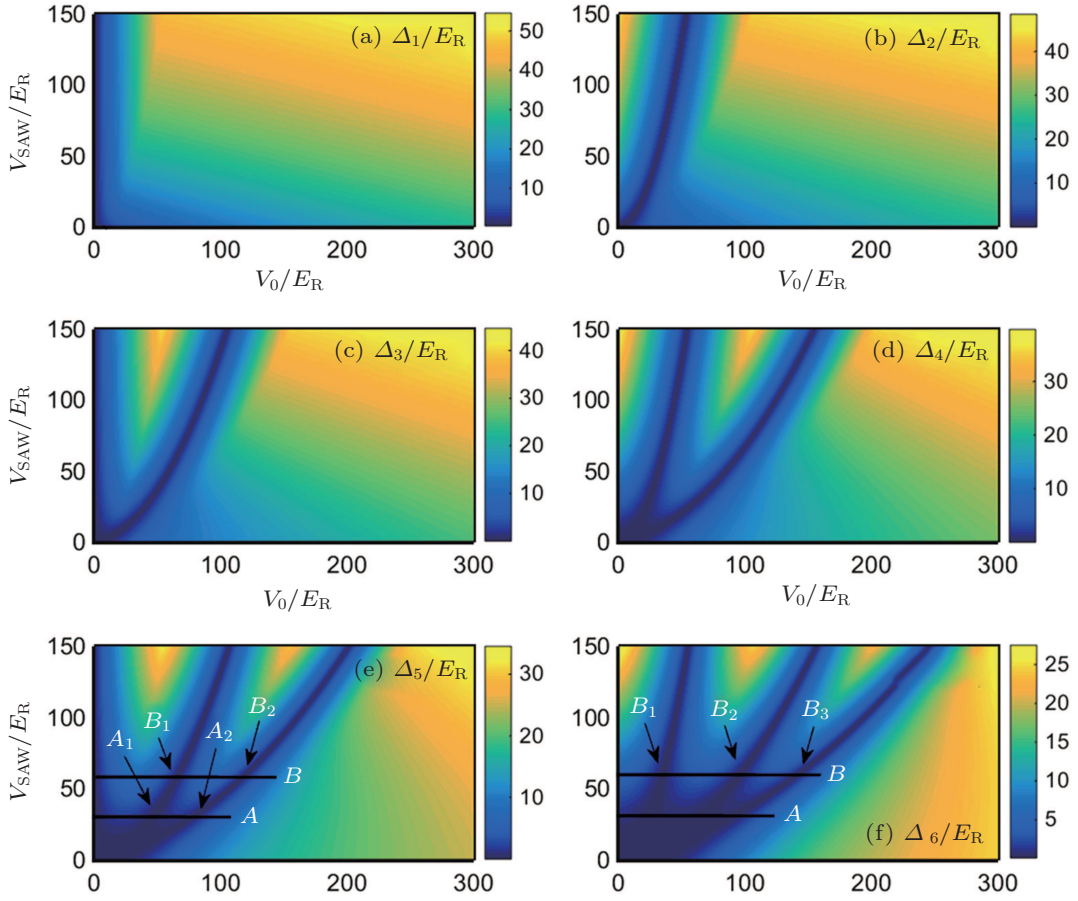


Fig. 3. (color online) Topographical map of the minimum energy gaps Δ_n ($n = 1$–6) versus V_0 and $V_{\rm SAW}$. The map is divided into several regimes by valleys where band gaps are closed. The rightmost region corresponds to the lowest plateaus of a pumping current of $I = 0ef$. The plateaus rise up from $0ef$ to nef (with an integer n) while we assign parameters from lower right areas to upper left ones.

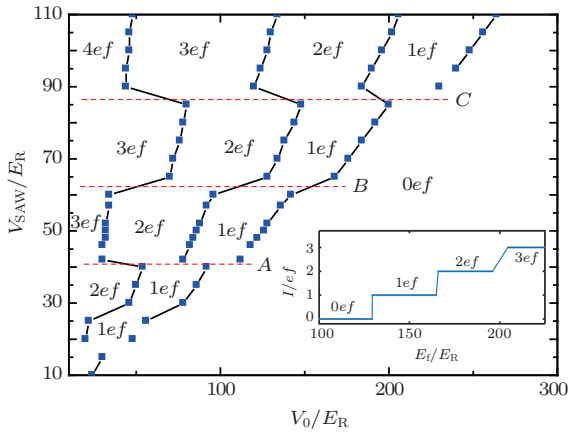


Fig. 4. (color online) Phase diagram of current plateaus versus V_0 and $V_{\rm SAW}$. Each region corresponds to the summation of Chern numbers of the filled bands. Inset: schematic plot of staircase-like pumping current versus the Fermi energy for $V_{\rm SAW} = V_0 = 100E_{\rm R}$.

Based on the above analysis, in Fig. 4 we summarize the current plateau diagram versus V_0 and $V_{\rm SAW}$. Each region is labeled by the summation of Chern numbers of the well-separated bands. The 'phase' boundary is determined by the closing point of the gaps. Deeper insights into the transitional issues at these boundaries are beyond the capability of topological interpretation. Experimentally, the boundary may be broadened due to thermal fluctuations. The gap must be large enough so that the insulating condition is satisfied. We argue that a partially-filled band has no contributions to the current induced by adiabatic pumping. Our theoretical treatment of non-interacting electrons qualitatively agrees with the experimental observations.[8,30]

4. Non-monotonous pumping plateaus by two SAWs

The performance of SAW in split gates without gate voltage is simply a sliding potential, which gives rise to the standard of particle pumping. An extended research has confirmed the equivalence between topological properties and quantized charge pumping of a continuous Rice–Mele pump.[19] In this section, we study the pumping effect of two sinusoidal SAWs with different spatial period but the same temporal frequency. The two SAWs have the same acoustic velocity. It can be realized by implementing an additional SAW propagating at an angle θ to the direction of the 1D channel. Explicitly, we consider the following SAW potential,

$$\tilde{V}_{\rm SAW}(x,t) = V_1\cos^2(\pi x/a - \omega t) + V_3\cos^2(3\pi x/a - \omega t). \quad (9)$$

The propagating angle of the first SAW is $\cos\theta = 1/3$.

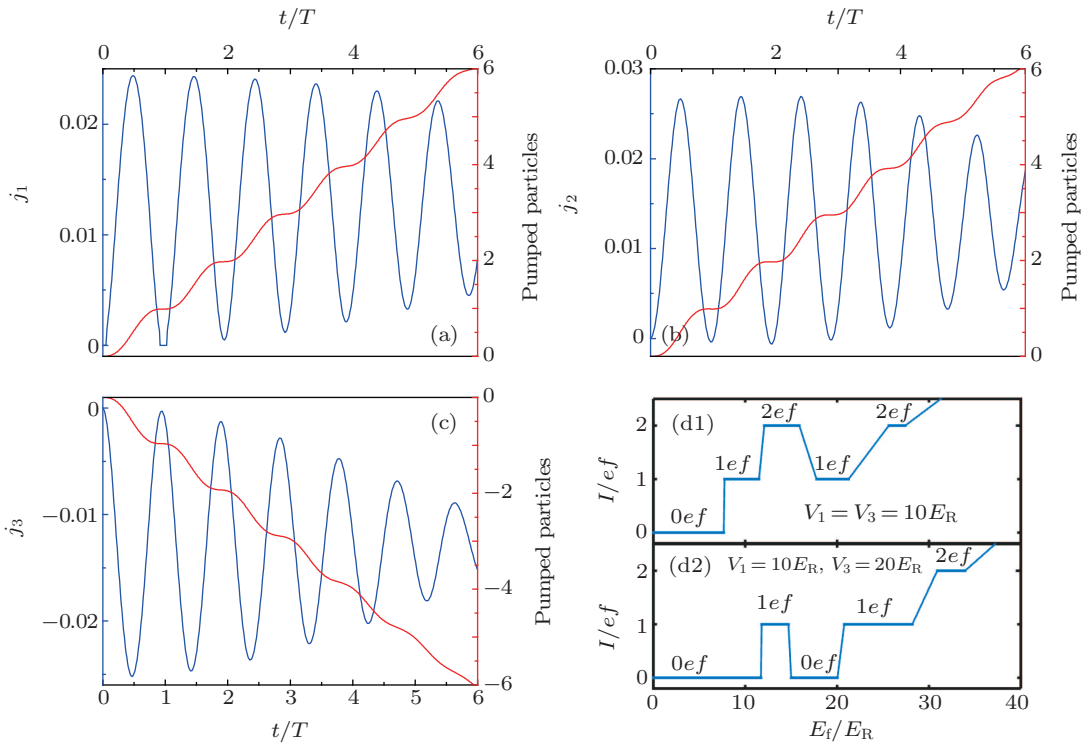


Fig. 5. (color online) Pumping currents (blue line) and particle number (red line) by the SAW potential (9) in panel (a) the first band, (b) the second band, and (c) the third band, respectively. Note that the pumping current is reversed in the third band, which is related to the Chern number $C_3 = -1$. (d) Non-monotonous current plateaus versus the Fermi energy for $V_1 = 10E_{\rm R}$. Upper panel (d1): $V_3 = 10E_{\rm R}$. Lower panel (d2): $V_3 = 20E_{\rm R}$.

The Chern number of each band can be computed in the same way. For $V_1 = V_3 = 10E_{\rm R}$, the Chern numbers of the lowest four bands are $C_n = 1, 1, -1, 1$. It is straightforward to calculate the current and pumped number of particles. Figure 5 shows the pumping currents of the three lowest bands. Each band contributes exactly one particle in an oscillating circle. Figure 5(c) indicates a pump in the negative direction, which corresponds to the Chern number $C_3 = -1$. The current plateaus are depicted according to the band structure and the Chern invariants, as shown in Fig. 5(d1). The pumping currents exhibit a non-monotonous rather than the staircase-like behavior. For $V_1 = 10E_{\rm R}$ and $V_3 = 20E_{\rm R}$ the Chern numbers of the lowest four bands are $C_n = 1, -1, 1, 1$. The pumping current is zero if the lowest two band are filled, as shown in Fig. 5(d2).

Finally, if we keep $V_1 = 30E_{\rm R}$ while increasing the second SAW amplitude from $V_3 = 30E_{\rm R}$ to $V_3 = 40E_{\rm R}$, we can observe a jump from the $I = 3ef$ plateau to the $I = 1ef$ plateau. In this case, the Chern numbers of the four lowest bands experience a transition from $C_n = 1, 1, 1, -1$ to $C_n = 1, 1, -1, 1$.

5. Summary

In summary, we have investigated the SAW pumping effects in a 1D channel with barrier potentials caused by the gate voltage. The quantized pumping of electrons is interpreted in the viewpoint of topological invariants of the filled bands. The jump between two adjacent current plateaus is related to a topological transition. One of the benefits of topological theory is that the quantized plateaus are robust against perturbations as long as the gap keeps finite. Based on our interpretation, we predicted non-monotonous current plateaus pumped by two homodromous SAWs. Our prediction can be readily verified by current experiment techniques.[31,32]

References

[1] Wixforth A, Scriba J, Wassermeier M, Kotthaus J P, Weimann G and Schlapp W 1989 *Phys. Rev. B* **40** 7874
[2] Barnes C, Shilton J and Robinson A 2000 *Phys. Rev. B* **62** 8410

[3] Shilton J, Talyanskii V, Pepper M, Ritchie D, Frost J, Ford C, Smith C and Jones G 1996 *J. Phys.: Condens. Matter* **8** L531
[4] Maksym P A 2000 *Phys. Rev. B* **61** 4727
[5] Robinson A M and Barnes C H W 2001 *Phys Rev. B* **63** 165418
[6] Chen X S. and Gao J 2010 *Solid State Commun.* **150** 91
[7] Galperin Y M, Entin-Wohlman O and Levinson Y 2001 *Phys. Rev. B* **63** 153309
[8] Ahlers F J, Fletcher N E, Ebbecke J and Janssen T J B M 2004 *Curr. Appl. Phys.* **4** 529
[9] Aharony A and Entin-Wohlman O 2002 *Phys. Rev. B* **65** 241401
[10] Kashcheyevs V, Aharony A and Entin-Wohlman O 2004 *Eur. Phys. J. B-Condens. Matter and Complex Systems* **39** 385
[11] Lang L J, Cai X and Chen S 2012 *Phys. Rev. Lett.* **108** 220401
[12] Hasan M Z and Kane C L 2010 *Rev. Mod. Phys.* **82** 3045
[13] Zheng Y J, Song J T and Li Y X 2016 *Chin. Phys. B* **25** 037301
[14] Liu Y, Zhao J Z Yu L, *et al.* 2015 *Chin. Phys. Lett.* **32** 067303
[15] Wray L A, Xu S Y, Xia Y, Hor Y S, Qian D, Fedorov A V, Lin H, Bansil A, Cava R J and Hasan M Z 2010 *Nat. Phys.* **6** 855
[16] Kitagawa T, Berg E, Rudner M and Demler E 2010 *Phys. Rev. B* **82** 235114
[17] Meidan D, Micklitz T and Brouwer P W 2010 *Phys. Rev. B* **82** 161303
[18] Wang L, Troyer M and Dai X 2013 *Phys. Rev. Lett.* **111** 026802
[19] Zheng Y and Yang S J 2014 *Physica B* **454** 93
[20] Leek P, Buitelaar M, Talyanskii V, Smith C, Anderson D, Jones G, Wei J and Cobden D 2005 *Phys. Rev. Lett.* **95** 256802
[21] Connolly M, Chiu K, Giblin S, Kataoka M, Fletcher J, Chua C, Griffiths J, Jones G, Fal'Ko V and Smith C 2013 *Nat. Nanotechnol.* **8** 417
[22] Thouless D J 1983 *Phys. Rev. B* **27** 6083
[23] Gumbs G, Aĭzin G and Pepper M 1999 *Phys. Rev. B* **60** 13954
[24] Nakahara M 2003 *Geometry, Topology and Physics*, 2nd edn. (London: Institute of Physics Publishing) pp. 428–437
[25] Berry M V 1984 *Proc. Royal Soc. Lond. A: Mathematical and Physical Sciences* **392** 45
[26] Wang Z C, Li L and Gao J 2004 *Phys. Lett. A* **331** 337
[27] Xiao D, Chang M C and Niu Q 2010 *Rev. Mod. Phys.* **82** 1959
[28] Flensberg K, Niu Q and Pustilnik M 1999 *Phys. Rev. B* **60** R16291
[29] Pustilnik M, Flensberg K and Niu Q 2000 *J. Low Temp. Phys.* **118** 571
[30] Fletcher N, Ebbecke J, Janssen T, Ahlers F, Pepper M, Beere H and Ritchie D 2003 *Phys. Rev. B* **68** 245310
[31] Shabani J, Kim Y, Lutchyn R and Nayak C 2014 *APS Meeting Abstracts* **1** 50003
[32] Bloch I 2005 *Nat. Phys.* **1** 23